

On the measurement of the thermal impedance in vertical-external-cavity surface-emitting lasers

J. Hader, T.-L. Wang, J. V. Moloney, B. Heinen, M. Koch et al.

Citation: *J. Appl. Phys.* **113**, 153102 (2013); doi: 10.1063/1.4802586

View online: <http://dx.doi.org/10.1063/1.4802586>

View Table of Contents: <http://jap.aip.org/resource/1/JAPIAU/v113/i15>

Published by the [American Institute of Physics](#).

Additional information on J. Appl. Phys.

Journal Homepage: <http://jap.aip.org/>

Journal Information: http://jap.aip.org/about/about_the_journal

Top downloads: http://jap.aip.org/features/most_downloaded

Information for Authors: <http://jap.aip.org/authors>

ADVERTISEMENT



AIPAdvances

Now Indexed in Thomson Reuters Databases

Explore AIP's open access journal:

- Rapid publication
- Article-level metrics
- Post-publication rating and commenting

On the measurement of the thermal impedance in vertical-external-cavity surface-emitting lasers

J. Hader,^{1,2} T.-L. Wang,² J. V. Moloney,^{1,2} B. Heinen,² M. Koch,³ S. W. Koch,³ B. Kunert,^{3,4} and W. Stolz^{3,4}

¹*Nonlinear Control Strategies Inc., 3542 N. Geronimo Ave., Tucson, Arizona 85705, USA*

²*College of Optical Sciences, University of Arizona, Tucson, Arizona 85721, USA*

³*Department of Physics and Material Sciences Center, Philipps Universität Marburg, Renthof 5, 35032 Marburg, Germany*

⁴*NAsP-III/V GmbH., Am Knechtacker 19, 35041 Marburg, Germany*

(Received 14 March 2013; accepted 3 April 2013; published online 18 April 2013)

A detailed and systematic analysis of the loss mechanisms in vertical-external-cavity surface-emitting lasers is presented with the goal to correctly determine the amount of pump power that is converted to heat. With this input, the accuracy of a recently proposed method for measuring the thermal impedance based on roll-over characteristics is shown to be very high for devices with and without dielectric coating. Potential errors arising from non-heating losses can be determined by performing experiments with different out-coupling mirrors. © 2013 AIP Publishing LLC
[\[http://dx.doi.org/10.1063/1.4802586\]](http://dx.doi.org/10.1063/1.4802586)

I. INTRODUCTION

In vertical-external-cavity surface-emitting lasers (VECSELs), the maximum achievable power is predominantly limited by heating due to non-radiative losses. With increasing temperature, the optical gain for a fixed carrier density decreases.¹ Thus, to maintain the needed gain, a higher carrier density is required which further increases the losses and heating. This self-perpetuating process is accelerated once Auger losses become important since these losses strongly increase with density. Ultimately, the device will shut off due to thermal roll-over.

In short-cavity lasers like VECSELs, the roll-over effects are accelerated since the heating also shifts the gain away from the wavelength selecting cavity resonance.^{2,3} Thus, heat management is particularly important in these systems.^{4,5} The quality of this management is characterized by the thermal impedance, R_{thr} , which measures the increase in temperature with heating power. Determining this quantity requires separating power losses that contribute to heating from those that do not. In the simplest approaches, it is assumed that the heating power is given by the difference between pump and output power. However, with this assumption, one ignores the fact that significant amounts of power are lost to intra-cavity scattering and spontaneous emission without contributing to heating.

Most traditional methods determine R_{thr} from the ratio between the power dependent and the temperature dependent wavelength changes. Here, the temperature dependence is determined by varying the heat sink temperature, T_{HS} and measuring either the shift of the lasing wavelength at a given pump or output power or the shift of the reflectivity or photo luminescence spectra at low pump power. The power dependence is determined by measuring the lasing wavelength as function of the pump intensity at a given T_{HS} . However, using low power spectral features is complicated in VECSELs due to the interplay of the wavelength selecting cavity resonance

and the underlying quantum well absorption/gain. Also, the reflectivity shifts vary depending on the selected wavelength since the corresponding modes are located predominantly in different parts of the structure made of different materials. At elevated powers, the question arises whether the intrinsic losses and, thus, the ratio between heating and non-heating power is the same at all T_{HS} and/or pump powers.

A method for determining R_{thr} in VECSELs without having to measure any spectral features has been proposed in Ref. 6. This method relies on the experimental observation that the intrinsic temperature at roll-over (maximum output power) is independent of T_{HS} . If this is correct, the thermal impedance can be determined by measuring the change of the heating power at roll-over, $P_{\text{heat}}^{\text{ro}}$ with T_{HS} ,

$$R_{\text{thr}} = \frac{\Delta T_{\text{HS}}}{\Delta P_{\text{heat}}^{\text{ro}}}. \quad (1)$$

This method dramatically simplifies the experimental procedure. Also, it could potentially increase the accuracy of the measurements since it eliminates many uncertainties of the shift-dependent methods.

Here, we use a systematic microscopic many-body theory to investigate the validity of the main assumption that the intrinsic temperature at roll-over is independent of T_{HS} . Like the shift-rate based methods, this model relies on an accurate determination of the heating power, P_{heat} . Therefore, we discuss the conversion of the net pump power into laser output power as well as heating and non-heating losses. We demonstrate how possible errors in the estimates of the respective contributions can be minimized for the roll-over method. Finally, we test whether this method can also be used on devices with anti-reflection (AR) coatings.

The VECSEL device investigated here consists of an active region with 10 InGaAs quantum wells, GaAsP pump absorbing barriers and a GaAs/AlAs distributed Bragg reflector (DBR) which is absorbent at the pump wavelength of

808 nm. The lasing wavelength varies from about 1019 nm at threshold to 1028 nm at roll-over. This device has recently been shown to yield record output powers over 100 W at temperatures around 0 °C.⁷

II. CARRIER LOSS MODEL

We use our fully microscopic theory to calculate the density and temperature dependent absorption/gain as well as the intrinsic carrier losses such as spontaneous emission (SE) and Auger losses.⁸ In this approach, electron-electron and electron-phonon scatterings are calculated explicitly solving quantum Boltzmann type scattering equations. Also, higher excitonic source terms are included in the calculation of the SE which has been shown to significantly influence the SE strength. All these models have been tested very successfully for various material systems, including AlInGaPAs based VECSELs as investigated here.^{8,9}

Using the microscopically calculated quantities as input for a semi-classical VECSEL model has been shown to yield very good agreement with the measured operating characteristics, like input-output power and lasing wavelength and their dependence on T_{HS} .^{8,10}

In general, the pump power, P_p , is converted in part into lasing output (P_{out}), heat (P_{heat}), and a remaining part that does not contribute to output or heating (P_{rest}),

$$P_p = P_{\text{out}} + P_{\text{heat}} + P_{\text{rest}}. \quad (2)$$

Several processes contribute to P_{heat} . First, in the device discussed here, that part of the pump power P_{NA} that is not absorbed in the active region, i.e., the part that reaches the DBR is absorbed there and converted into heat. Second, carriers created via pump absorption relax to the bottom of the quantum wells. In doing so, they give their excess energy—the so-called quantum defect— P_{QD} , as heat to the lattice via phonon emission.

Other contributions to heating are losses due to Auger and defect recombination, P_{aug} and P_d , respectively. The density- and temperature-dependent Auger recombination time, τ_{aug} , is calculated explicitly. For defect losses, we assume a recombination time $\tau_d = 100$ ps, which is typical for material of the quality as investigated here.

A final source of heating arises from that part of the SE that is emitted in the quantum-wells and then re-absorbed outside the pump spot. This part depends on the pump spot size and heat extraction efficiency whether the heating occurring there also influences the center of the pump spot where thermal roll-over is usually initiated.¹¹ The balance between the SE-power effectively contributing to heating, $P_{\text{SE-H}}$, and not, $P_{\text{SE-NH}}$, can be estimated using ray tracing. Here, we use the ratio as an adjustable parameter with values based on such estimates.

Besides $P_{\text{SE-NH}}$, a second loss mechanism that does not contribute to heating is intra-cavity surface scattering. At each cavity round-trip, some of the lasing light will be reflected on height fluctuations of the semiconductor interfaces. This leads to a power loss due to destructive interference, $P_{\text{SS}} = P_{\text{out}}\alpha_{\text{SS}}/\alpha_{\text{out}}$. Here, α_{out} is the out-coupling loss

and α_{SS} is the surface scattering loss. Since the surface scattering depends on the growth- and processing quality, it cannot be calculated *a priori*. Thus, we treat α_{SS} as an adjustable parameter.

In principal, there can be additional losses that also do not contribute to heating like diffraction losses due to thermal lensing or scattering at interfaces inside the semiconductor material. These contribute to the power balance just like the surface scattering losses described above. In our model, these losses are also included via the scattering parameter α_{SS} .

Equations (3) and (4) summarize the balance of powers. Here, $W = Nn_wA_p\hbar\omega_L$, where N is the sheet carrier density, n_w the number of wells, A_p the pumped area, $\hbar\omega_L$ the lasing energy, and $\hbar\omega_p$ the pump energy. η_{SE} is the fraction of SE not contributing to heating. η_{abs} is the fraction of pump light that is absorbed in the active region,

$$P_{\text{heat}} = P_{\text{NA}} + P_{\text{QD}} + P_{\text{aug}} + P_d + P_{\text{SE-H}} \\ = P_p - \eta_{\text{abs}} \frac{\hbar\omega_L}{\hbar\omega_p} P_p + W \left[\frac{1}{\tau_d} + \frac{1}{\tau_{\text{aug}}} + \frac{1 - \eta_{\text{SE}}}{\tau_{\text{SE}}} \right], \quad (3)$$

$$P_{\text{rest}} = P_{\text{SS}} + P_{\text{SE-NH}} = P_{\text{out}} \frac{\alpha_{\text{SS}}}{\alpha_{\text{out}}} + \frac{W\eta_{\text{SE}}}{\tau_{\text{SE}}}. \quad (4)$$

To calculate the VECSEL operating characteristics, it has been shown to be sufficient to use a one-dimensional model⁸ where lateral inhomogeneities are neglected. Thus, the output power scales linearly with the pumped area. This model has been shown to give very good agreement with the experiment especially for large pump spots and multi mode operation conditions.^{8,10} All together, the microscopic model used here not only provides a high quantitative accuracy but also reduces the number of adjustable parameters to a minimum. The only such parameters left are α_{SS} , η_{SE} and R_{thr} .

III. RESULTS

For the experiment investigated here, we find the best experiment-theory agreement using $R_{\text{thr}} = 1.24$ K/W, $\eta_{\text{SE}} = 85\%$, and $\alpha_{\text{SS}} = 0.57\%$. There is some ambiguity in the fitting process. Fairly, similar results can be obtained, e.g., using $\eta_{\text{SE}} = 75\%$ and $R_{\text{thr}} = 1.22$ K/W or $\eta_{\text{SE}} = 100\%$ and $R_{\text{thr}} = 1.26$ K/W while keeping $\alpha_{\text{SS}} = 0.57\%$. The ambiguity is limited since the parameters influence different characteristics differently. R_{thr} predominantly determines the maximum power while it has minimal impact on threshold and efficiency. α_{SS} mainly influences the efficiency. η_{SE} has a weak influence on all three characteristics. This allows us to determine the parameters individually with high accuracy. Here, we estimate the uncertainty margins to be less than about 25% for η_{SE} and α_{SS} and 5% for R_{thr} .

Fig. 1 shows the measured and calculated operating characteristics for $T_{\text{HS}} = 10$ °C, a pump spot diameter of 0.92 mm and an out-coupling mirror loss of 3.0%. Included in Fig. 1 are the calculated individual loss contributions. The non-heating losses, P_{rest} , are quite significant. Not considering them correctly and instead assuming that P_{heat} is given by $(P_p - P_{\text{out}})$ would lead to a significant over-estimation of

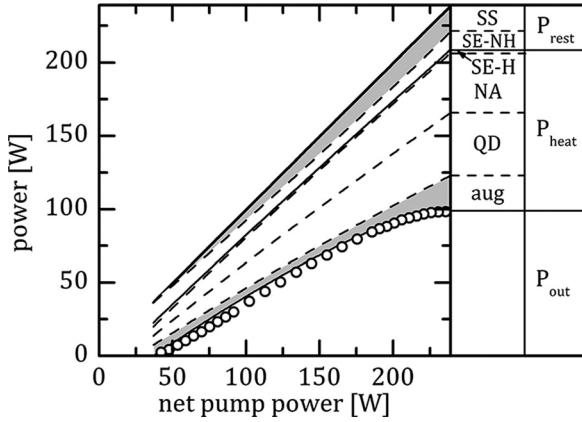


FIG. 1. Distribution of the net pump power over various mechanisms contributing to P_{out} , P_{heat} , and P_{rest} at $T_{HS} = 10^\circ\text{C}$. Dots: Experimentally measured P_{out} . Lines: Theory. Shaded areas: Losses due to Auger and surface scattering. Not shown here is P_d which is too small to resolve.

P_{heat} and, thus, R_{thr} . Here, the error would be about a factor of 1.75 at threshold and 1.25 at roll-over.

Particularly important for the following analysis is also that the contribution to P_{rest} from SE, P_{SE-NH} does not depend on pump power. On the other hand, since the scattering loss is proportional to the output power, it increases with pump power up to the roll-over point. We generally find the variation of P_{rest} with P_p to be dominated by that of P_{SS} . The variation is particular strong in cases with low out-coupling losses since then the scattering loss is more pronounced.

For the validity of the roll-over method, it is crucial that the intrinsic temperature at roll-over is independent of the heat sink temperature. In the experimental work,⁶ this assumption is based on the observation that the lasing wavelength appears to be independent of T_{HS} within the scattering of the experimental data. Here, we use the microscopic modeling to test this feature.

Fig. 2 shows the calculated lasing wavelength and intrinsic temperature as function of the pump power for various T_{HS} . We see that the lasing wavelength at roll-over decreases minimally with T_{HS} by about 0.025 nm/K, nicely confirming the experimental conclusions. The intrinsic temperature decreases about 0.016 K per Kelvin heat sink change. For the derived thermal impedances, this introduces an error of about 2%.

Fig. 3 shows the measured and calculated dissipated power at roll-over as function of T_{HS} . According to Eq. (1),

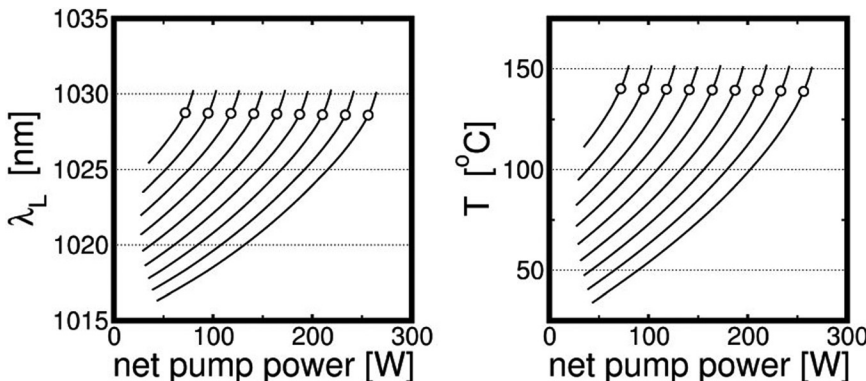


FIG. 2. Lasing wavelength (left) and internal temperature (right) as function of P_p between threshold and shut-off for $T_{HS} = 0, 10, \dots, 80^\circ\text{C}$. Dots: roll-over point.

the thermal impedance is simply given by the presumably constant slope of the data. Within the scattering of the data, the slope is indeed constant. For the calculated results, the slope agrees with the modeling value of $R_{thr} = 1.24 \text{ K/W}$ when the correct heating power is used. In the experiment, the heating power is generally not known, but $(P_p - P_{out})$ can be easily determined. When using that, one also finds a linear dependence, but the slope under-estimates the thermal impedance. Using this in the modeling yields $R_{thr} = 0.99 \text{ K/W}$.

The modeling results show good agreement with the experiment when using $(P_p - P_{out})$ in both cases. The deviations between theoretical and experimental result are more or less within the scattering of the experimental data. Some uncertainty arises in the experiment due to the often somewhat unclear determination of the exact roll-over point. Here, the experimental data fall in between the theoretical data for roll-over and shut-off.

The error when using $(P_p - P_{out})$ instead of P_{heat} is mostly due to the power dependence of the scattering loss. Thus, the error can be reduced by reducing the influence of the surface scattering. This can be done by using an out-coupling mirror with a higher loss.

Fig. 4 shows the theoretical results of the roll-over method for varying out-coupling losses. We see that the error of using $(P_p - P_{out})$ is reduced significantly for large out-coupling losses. In the limit of high losses, the data agree rather well with that for the case that uses the correct heating power.

The modeling data show some scattering and tends to yield values for R_{thr} slightly above the actual input value. The scattering is due to the errors introduced by the discrete density and temperature grids used for the microscopically calculated data. The slight over-estimation of R_{thr} is due to the residual shift of the intrinsic temperatures with heat sink temperature.

Finally, we test the roll-over method for an AR coated device. With such a coating, the cavity enhancement of the gain is strongly reduced and the position and shifts of the lasing wavelength are mostly given by the shift of the material gain maximum rather than the cavity resonance. Thus, the limiting factor is the available maximum material gain rather than the gain at the position of the cavity resonance wavelength. The question arises whether this allows for the shut-off to occur at heat-sink temperature dependent intrinsic conditions, or, as required by the roll-over method, at a heat sink temperature independent intrinsic temperature. To test

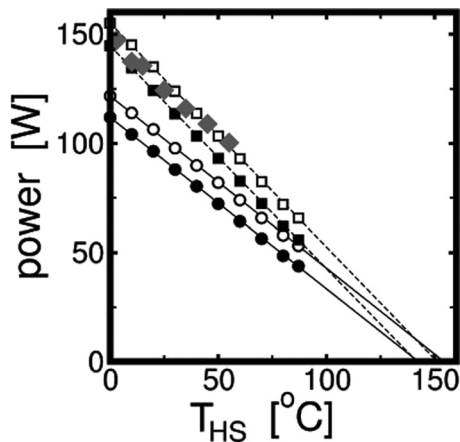


FIG. 3. Dissipated power at roll-over as function of T_{HS} . Diamonds: Experimental data, assuming the dissipated power is given by $(P_p - P_{out})$. Circles: Theory for P_{heat} . Squares: Theory for $(P_p - P_{out})$. Closed symbols: Data at roll-over. Open symbols: At shut-off. Lines: linear interpolation.

this, we assume that a quarter wavelength dielectric coating of Si_3N_4 has been deposited on the VECSEL. Since the achievable modal gain is reduced by the coating, an out-coupling mirror with a lower loss has to be used. Here, we assume an out-coupling mirror with a 1% loss. The coating also reduces surface scattering losses, typically by about 50%.⁸ Therefore, we assume a scattering loss of only 0.29% as compared to 0.57% without coating. All other parameters are kept the same as for the uncoated device.

Fig. 5 shows the results of the roll-over method for the AR-coated device. We see that the method works here almost as well as in the uncoated case. If the correct heating power is known, the slope of the data is about 1.28 K/W, very close to the used value of $R_{thr} = 1.24$ K/W.

Due to the smaller out-coupling loss, the influence of the surface scattering loss is more pronounced. As has been shown in Fig. 4 for the uncoated device, this leads to a larger error when using $(P_p - P_{out})$ instead of P_{heat} . Here, this would yield $R_{thr} = 0.90$ K/W. The error is somewhat limited since the coating reduces the scattering losses. As for the uncoated device, an estimate for the error can be obtained by

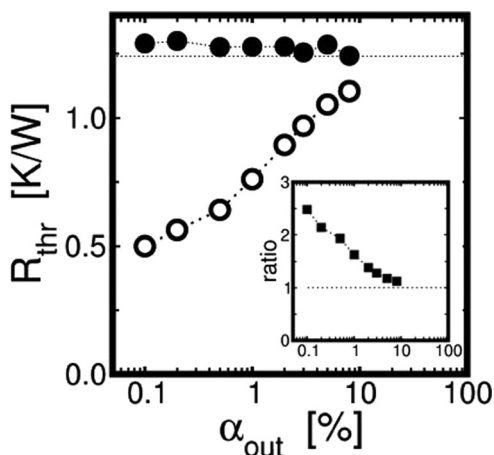


FIG. 4. Thermal impedance calculated for various out-coupling losses. Solid dots: Using P_{heat} . Open dots: Using $(P_p - P_{out})$. Dotted line: value used in the modeling. Inset: Ratio by which R_{thr} is over-estimated when using $(P_p - P_{out})$.

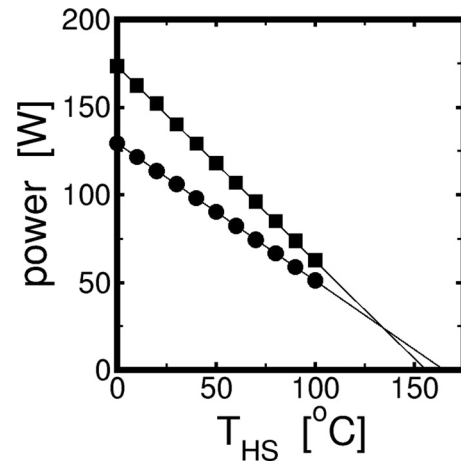


FIG. 5. Dissipated power at roll-over as function of T_{HS} for an AR-coated device. Squares: Assuming the dissipated power is given by $(P_{pump} - P_{out})$. Circles: Data for P_{heat} . Lines: linear interpolation.

varying the out-coupling loss. However, the AR-coated device can only sustain losses up to about 2.5%.

IV. SUMMARY

In summary, our microscopic many-body analysis verifies that the intrinsic temperature at roll-over in VECSELs is independent of the heat sink temperature, thus validating that the thermal impedance can be uniquely determined from roll-over characteristics.⁶ We demonstrate that this method can be applied to coated and uncoated devices.

ACKNOWLEDGMENTS

This work was supported by the U.S. Air Force Office of Scientific Research, contracts FA9550-10-1-0064, FA8650-11-C-1009 P00002, and FA9550-13-C-0009, the Deutsche Forschungsgemeinschaft and the Humboldt Foundation.

¹M. Mangold, V. J. Wittwer, O. D. Sieber, M. Hoffmann, I. L. Krestnikov, D. A. Livshits, M. Golling, T. Südmeyer, and U. Keller, *Opt. Express* **20**, 4136 (2012).

²A. C. Topper, H. D. Foreman, A. Garnache, K. G. Wilcox, and S. H. Hoogland, *J. Phys. D: Appl. Phys.* **37**, R75 (2004).

³N. Schulz, M. Rattunde, C. Ritzenthaler, B. Rosner, C. Manz, K. Kohler, and J. Wagner, *IEEE Photon Technol. Lett.* **19**, 1741 (2007).

⁴A. J. Kemp, J.-M. Hopkins, A. J. Maclean, N. Schulz, M. Rattunde, J. Wagner, and D. Burns, *IEEE J. Quantum Electron.* **44**, 125 (2008).

⁵S. L. Vetter and S. Calvez, *IEEE J. Quantum Electron.* **48**, 345 (2012).

⁶B. Heinen, F. Zhang, M. Sparenberg, B. Kunert, M. Koch, and W. Stolz, *IEEE J. Quantum Electron.* **48**, 934 (2012).

⁷B. Heinen, T.-L. Wang, M. Sparenberg, A. Weber, B. Kunert, J. Hader, S. W. Koch, J. V. Moloney, M. Koch, and W. Stolz, *Electron. Lett.* **48**, 516 (2012).

⁸J. Hader, T.-L. Wang, M. J. Yarborough, C. A. Dineen, Y. Kaneda, J. V. Moloney, B. Kunert, W. Stolz, and S. W. Koch, *IEEE J. Sel. Top. Quantum Electron.* **17**, 1753 (2011).

⁹T.-L. Wang, B. Heinen, J. Hader, C. Dineen, M. Sparenberg, A. Weber, B. Kunert, S. W. Koch, J. V. Moloney, M. Koch, and W. Stolz, *Laser Photonics Rev.* **6**, L12 (2012).

¹⁰J. Hader, G. Hardesty, T.-L. Wang, M. J. Yarborough, Y. Kaneda, J. V. Moloney, B. Kunert, W. Stolz, and S. W. Koch, *IEEE J. Quantum Electron.* **46**, 810 (2010).

¹¹A. Chernikov, J. Herrmann, M. Scheller, M. Koch, B. Kunert, W. Stolz, S. Chatterjee, S. W. Koch, T.-L. Wang, Y. Kaneda, J. M. Yarborough, J. Hader, and J. V. Moloney, *Appl. Phys. Lett.* **97**, 191110 (2010).